Monthly Notices
of the
ROYAL ASTRONOMICAL SOCIETY

MNRAS **480,** 3879–3888 (2018)
Advance Access publication 2018 July 20

doi:10.1093/mnras/sty1939

# Dark Energy Survey Year 1 Results: A Precise $H_0$ Estimate from DES Y1, BAO, and D/H Data

T. M. C. Abbott,[1] F. B. Abdalla,[2,3] J. Annis,[4] K. Bechtol,[5] J. Blazek,[32,55] B. A. Benson,[4,6,7] R. A. Bernstein,[8] G. M. Bernstein,[9] E. Bertin,[10,11] D. Brooks,[3] D. L. Burke,[12,13] A. Carnero Rosell,[14,15] M. Carrasco Kind,[16,17] J. Carretero,[18] F. J. Castander,[19] C. L. Chang,[6,7,20] T. M. Crawford,[6,7] C. E. Cunha,[12] C. B. D'Andrea,[9] L. N. da Costa,[14,15] C. Davis,[12] J. DeRose,[12,53] S. Desai,[21] H. T. Diehl,[4] J. P. Dietrich,[22,23] P. Doel,[3] A. Drlica-Wagner,[4] A. E. Evrard,[24,25] E. Fernandez,[18] B. Flaugher,[4] P. Fosalba,[19] J. Frieman,[4,7] J. García-Bellido,[26] E. Gaztanaga,[19] D. W. Gerdes,[24,25] T. Giannantonio,[27,28,29] D. Gruen,[12,13] R. A. Gruendl,[16,17] J. Gschwend,[14,15] G. Gutierrez,[4] W. G. Hartley,[3,30] J. W. Henning,[6,7] K. Honscheid,[31,32] B. Hoyle,[27,33] D. Huterer,[25] B. Jain,[9] D. J. James,[34] M. Jarvis,[9] T. Jeltema,[35] M. D. Johnson,[17] M. W. G. Johnson,[17] E. Krause,[36] K. Kuehn,[37] S. Kuhlmann,[38] N. Kuropatkin,[4] O. Lahav,[3] A. R. Liddle,[39] M. Lima,[15,40] H. Lin,[4] N. MacCrann,[31,32] M. A. G. Maia,[14,15] A. Manzotti,[41] M. March,[9] J. L. Marshall,[42] R. Miquel,[18,43] J. J. Mohr,[22,23,33] T. Natoli,[44] P. Nugent,[45] R. L. C. Ogando,[14,15] Y. Park,[46] A. A. Plazas,[36] C. L. Reichardt,[47] K. Reil,[13] A. Roodman,[12,13] A. J. Ross,[32] E. Rozo,[46] E. S. Rykoff,[12,13] E. Sanchez,[48] V. Scarpine,[4] M. Schubnell,[25] D. Scolnic,[7] I. Sevilla-Noarbe,[48] E. Sheldon,[54] M. Smith,[49] R. C. Smith,[1] M. Soares-Santos,[4] F. Sobreira,[15,50] E. Suchyta,[51] G. Tarle,[25] D. Thomas,[52] M. A. Troxel,[31,32] A. R. Walker,[1] R. H. Wechsler,[12,13,53] J. Weller,[23,27,33] W. Wester,[4] W. L. K. Wu,[7] J. Zuntz[39] and (The Dark Energy Survey and the South Pole Telescope Collaborations)★

*Affiliations are listed at the end of the paper*

Accepted 2018 July 17. Received 2018 July 17; in original form 2017 November 16

**ABSTRACT**

We combine Dark Energy Survey Year 1 clustering and weak lensing data with baryon acoustic oscillations and Big Bang nucleosynthesis experiments to constrain the Hubble constant. Assuming a flat ΛCDM model with minimal neutrino mass ($\sum m_\nu = 0.06$ eV), we find $H_0 = 67.4^{+1.1}_{-1.2}$ km s$^{-1}$ Mpc$^{-1}$ (68 per cent CL). This result is completely independent of Hubble constant measurements based on the distance ladder, cosmic microwave background anisotropies (both temperature and polarization), and strong lensing constraints. There are now five data sets that: (a) have no shared observational systematics; and (b) each constrains the Hubble constant with fractional uncertainty at the few-per cent level. We compare these five independent estimates, and find that, as a set, the differences between them are significant at the 2.5$\sigma$ level ($\chi^2/dof = 24/11$, probability to exceed = 1.1 per cent). Having set the threshold for consistency at 3$\sigma$, we combine all five data sets to arrive at $H_0 = 69.3^{+0.4}_{-0.6}$ km s$^{-1}$ Mpc$^{-1}$.

**Key words:** cosmological parameters – cosmology: observations – distance scale.

★ E-mail: des-publication-queries@fnal.gov

## 1 INTRODUCTION

The current standard model of cosmology is remarkably successful. With only six free parameters, it can accurately describe the entire history of the Universe. The variety of data fit by this remarkable model includes primordial light element abundances (e.g. Cooke et al. 2016, hereafter C16); the temperature and polarization angular power spectra of the cosmic microwave background (CMB) anisotropies (e.g. Planck Collaboration 2015; Henning et al. 2018); the distance–redshift relation of standard candles such as Type Ia supernovae (SNe) (e.g. Betoule et al. 2014); galaxy–galaxy (gg) clustering in the late-time Universe (e.g. Gaztañaga, Cabré & Hui 2009; Beutler et al. 2011; Ross et al. 2015; Alam et al. 2017); the time delays of multiply imaged quasars (e.g. Bonvin et al. 2017); and weak gravitational lensing measurements (e.g. Mandelbaum et al. 2013; Alsing, Heavens & Jaffe 2017; DES Collaboration 2017; Hildebrandt et al. 2017; Troxel et al. 2017; van Uitert et al. 2017).

Despite its tremendous success and its remarkable simplicity, the standard model of cosmology is theoretically surprising. In this model, ≈85 per cent of the matter in the Universe is dark matter, detected only through its gravitational impact on observable matter. Additionally, the current accelerating expansion of the Universe requires ≈70 per cent of the energy in the Universe to take the form of either a cosmological constant, a dynamical field with negative pressure, or a modification of general relativity. While the cosmological constant is usually viewed as the most conservative solution to this theoretical challenge, its interpretation as a manifestation of vacuum energy leads to naive predictions that differ from the observed value by many orders of magnitude (Weinberg 1989).

In short, the standard model of cosmology has provided indirect evidence of not one but two distinct extensions of the standard model of particle physics. It is therefore reasonable to expect that any cracks in this standard cosmological model might herald yet another surprise in our understanding of the cosmos.

One such possible crack arises from the value of the Hubble constant, i.e. the current rate of expansion of the Universe. The Hubble constant can be directly measured using Type Ia SNe, whose luminosities are calibrated using SNe hosted by nearby galaxies with known distances. Alternatively, measurements of the CMB indirectly constrain the Hubble constant via its impact on the CMB anisotropies. Both of these measurements are remarkably precise. Currently, the most precise SN measurement of the Hubble constant is that of the SH0ES collaboration, most recently updated in the work by Riess et al. (2018). They report $H_0 = 73.52 \pm 1.62\,\mathrm{km\ s^{-1}Mpc^{-1}}$. This value is in excellent agreement with that of Freedman et al. (2012, $H_0 = 74.3 \pm 1.5 \pm 2.1\,\mathrm{km\ s^{-1}Mpc^{-1}}$) and is to be compared to that inferred from *Planck* measurements assuming a flat ΛCDM model with minimal neutrino mass, $H_0 = 67.3 \pm 1.0\,\mathrm{km\ s^{-1}Mpc^{-1}}$ (*Planck* TT + low-*l* only). These two values are discrepant at $3.3\sigma$.[1] This difference provides a strong motivation for searching for alternative methods of measuring the Hubble constant (Freedman 2017).

As first highlighted by Addison, Hinshaw & Halpern (2013) and Aubourg et al. (2015), the baryon acoustic oscillation (BAO) signature in the clustering of galaxies provides a standard ruler that enables us to determine $H_0$ in a way that is independent of CMB anisotropies. The argument is as follows: Slight density fluctuations in the early universe launched sound waves at the epoch of the Big Bang. These sound waves travelled through the photon–baryon plasma until the epoch of decoupling, at which point the waves were no longer pressure supported and stalled. The distance travelled by these waves before stalling – the so-called sound horizon $r_\mathrm{s}$ – can be readily computed a priori for any set of cosmological parameters. The overdensities due to these sound waves seeded galaxy formation, leading to a bump in the galaxy correlation function at distances equal to the sound horizon $r_\mathrm{s}$. This bump is the so-called BAO feature.

Observationally, the BAO feature allows us to measure either the angle spanned by the distance $r_\mathrm{s}$ – leading to a constraint on $D_\mathrm{M}/r_\mathrm{s}$ – or the redshift interval corresponding to two galaxies separated by a distance $r_\mathrm{s}$ along the line of sight – leading to a constraint on $cH^{-1}/r_\mathrm{s}$. Here, $D_\mathrm{M}$ is the comoving angular diameter distance to the galaxies in question, and $H(z)$ is the Hubble expansion rate at the redshift of the observed galaxies. In a flat ΛCDM model, the Hubble rate is primarily sensitive to the Hubble constant $H_0$ – typically parametrized via $h$, where $H_0 = 100h\ \mathrm{km\ s^{-1}Mpc^{-1}}$ – and the total matter density parameter $\Omega_\mathrm{m}$. As an integral over the Hubble rate, these parameters also govern the behaviour of the angular diameter distance $D_\mathrm{M}$. Finally, the sound horizon $r_\mathrm{s}$ depends on: (1) the mean temperature of the CMB; (2) the dark matter density $\Omega_\mathrm{dm}h^2$, and (3) the baryon density $\Omega_\mathrm{b}h^2$. In practice, the precision with which the mean CMB temperature is known is already sufficiently high that we may ignore its observational uncertainties.

In summary, assuming the CMB temperature is known, and *within the context of a flat ΛCDM cosmology*, the BAO observables $D_\mathrm{M}/r_\mathrm{s}$ and $cH^{-1}/r_\mathrm{s}$ fundamentally depend on three key cosmological parameters only: $\Omega_\mathrm{m}$, $\Omega_\mathrm{b}h^2$, and $h$. BAO measurements at a single redshift will necessarily result in strong degeneracies between these parameters. Fortunately, the sensitivity of the sound horizon $r_\mathrm{s}$ to $\Omega_\mathrm{b}h^2$ is relatively mild ($d\ln r_\mathrm{s}/d\ln \Omega_\mathrm{b}h^2 \approx 0.13$, Aubourg et al. 2015), so even modest independent (i.e. non-BAO) constraints on $\Omega_\mathrm{b}h^2$ suffice to break the $\Omega_\mathrm{b}h^2$ degeneracy.

Big Bang nucleosynthesis (BBN) enables us to measure $\Omega_\mathrm{b}h^2$ through its impact on the primordial deuterium-to-hydrogen ($D/H$) ratio. During BBN, deuterium is burned to create $^4$He. The reaction rate increases with increasing baryon density, so $D/H$ decreases monotonically with $\Omega_\mathrm{b}h^2$.[2] The current best method for determining the primordial $D/H$ ratio relies on extremely low-metallicity line of sight to quasars, as determined from the quasar absorption spectrum. Such pristine lines of sight are unpolluted by baryonic processes in stars, so their element abundance ratios are expected to be primordial. Measurements of damped Ly $\alpha$ systems in the quasar absorption spectra are used to infer the $D/H$ ratio along these lines of sight, which in turn enables us to infer $\Omega_\mathrm{b}h^2$.

Even after including BBN data, a single BAO measurement will exhibit a strong $\Omega_\mathrm{m}$–$h$ degeneracy. This degeneracy ellipse rotates as the redshift is varied, so two BAO measurements that span a large redshift range can break this degeneracy. Aubourg et al. (2015) and

[1] Throughout this work, we rely exclusively on *Planck* TT + low-*l* polarization data. This ensures the *Planck* data set is independent of the SPTpol data set (Henning et al. 2018). Including high-*l* *Planck* polarization data increases the discrepancy between *Planck* and SH0ES to $3.8\sigma$, as quoted in Riess et al. (2016). However, Planck Collaboration (2015) found evidence for instrumental systematics in their high-*l* polarization spectra and urge caution while interpreting features in them.

[2] Here, we follow Planck Collaboration (2015) and focus exclusively on $D/H$ observations because of the more difficult nature of the observations and interpretation of other light elements, e.g. lithium (for a review, see Fields, Molaro & Sarkar 2014).

Addison et al. (2017, henceforth referred to as A17) combined low-redshift galaxy BAO measurements with high-redshift Ly $\alpha$ BAO data to arrive at an estimate of $h$ *when assuming a flat* $\Lambda CDM$ *cosmology*. A17 found $H_0 = 67.4 \pm 1.3\,\mathrm{km\,s^{-1}Mpc^{-1}}$, though the authors also note that there is a $\approx 2\sigma$ difference between the galaxy and Ly $\alpha$ BAO measurements.[3]

In this work, we break the $\Omega_m$–$h$ degeneracy of the galaxy BAO+BBN estimate of $H_0$ with clustering and weak lensing data from the Dark Energy Survey (DES) Year 1 data set. In DES Collaboration (2017), we have shown that our analysis of the DES Y1 data results in the most accurate and precise constraints on the total matter density $\Omega_m$ from any lensing analysis to date. In combination with galaxy BAO measurements and BBN constraints derived from *D*/*H* observations, we derive remarkably tight constraints on the Hubble rate that are independent of both CMB anisotropies and local supernova measurements. Throughout this work, we adopt $3\sigma$ (0.27 per cent) as the threshold for 'evidence of tension' and the usual $5\sigma$ ($5.7 \times 10^{-7}$) threshold for 'definitive evidence of tension', though we recognize these thresholds are necessarily subjective.

## 2 ANALYSIS

Our analysis relies on four sets of data:

(i) The *COBE*/FIRAS measurements of the temperature of the CMB (Fixsen 2009).

(ii) Galaxy BAO measurements from a variety of spectroscopic surveys.

(iii) Observational estimates of the primordial *D*/*H* ratio.

(iv) Tomographic shear, gg-lensing, and gg-clustering data on linear scales measured in the DES Y1 data set.

Our BAO constraints are taken directly from the constraints derived from the 6dF galaxy survey (Beutler et al. 2011), the SDSS Data Release 7 Main Galaxy sample (Ross et al. 2015), and the BOSS Data Release 12 (Alam et al. 2017). The 6dF and SDSS Main analyses were based on the monopole of the anisotropic galaxy correlation function and therefore do not constrain $D_M/r_s$ and $cH^{-1}/r_s$ individually; rather, they constrain the combination $D_V = [D_M^2 cz H^{-1}]^{1/3}$. Our BAO priors are listed in Table 1. Our default analysis does not include BAO constraints from Ly $\alpha$ measurements, though including them does not impact our conclusions in any way. As noted earlier, A17 combined galaxy and Ly $\alpha$ BAO to measure $H_0$ to high precision, though the mild ($2.4\sigma$) tension between the two BAO measurement suggests that an independent analysis that confirms their results would help strengthen the argument for a 'low' value for the Hubble constant. This is what DES can provide. For further discussion, see Section 4.

Our BBN priors are taken from the recent analysis by C16. Adopting the CMB temperature of Fixsen (2009), C16 reports two separate constraints on $\Omega_b h^2$: one obtained using a theoretical calculation for the $d(p,\gamma)^3$He reaction rate, and another obtained using experimental constraints for the same rate. The two results are discrepant at $3.5\sigma$. We adopt a conservative prior that places the central value of $\Omega_b h^2$ halfway between the two values reported in C16. The corresponding uncertainty is set to half the difference between the two results. Our BBN prior is reported in Table 1. We note that because of the mild sensitivity of the sound horizon $r_s$ to the baryon density $\Omega_b h^2$, even a perfect measurement of $\Omega_b h^2$ would not improve the posterior of our Hubble constant measurement in any appreciable way.

Finally, we use the likelihood framework described in Krause et al. (2017) to analyse the clustering of redMaGiC galaxies (Rozo et al. 2016; Elvin-Poole et al. 2017), the shear profile around redMaGiC galaxies (Prat et al. 2017), and the tomographic cosmic shear signal in the DES Y1 data (Troxel et al. 2017). The shear profile and cosmic shear analyses rely on the shape catalogues described in Zuntz et al. (2017), and the photometric redshift analyses in Hoyle et al. (2017). The latter include extensive validation of photometric redshift uncertainties via cross-correlation methods (Davis et al. 2017; Gatti et al. 2017; Cawthon et al. 2017). We refer the reader to these papers for a detailed description of the likelihood, data vectors, and robustness and systematics checks of the DES data. The entire framework was tested in simulations as described in MacCrann et al. (2018). The DES priors employed and the corresponding DES posteriors are presented in DES Collaboration (2017). These priors include a broad top hat prior on both the matter density ($\Omega_m \in (0.1, 0.9)$) and Hubble constant ($h \in (0.55, 0.90)$). Neither prior is important after combining with the BAO and BBN data. Both the BBN and DES analyses were performed blind, with all analyses choices fixed prior to revealing cosmological constraints (Cooke et al. 2016; DES Collaboration 2017). There are also no parameter or configuration choices made by us when performing this analysis: we are simply combining BBN, BAO, and DES data as published. Our treatment of the DES covariance matrix accounts for the effects of source clustering as described in Troxel et al. (2018).

**Table 1.** BAO and BBN priors, and DES data sets used in this analysis. The BOSS BAO priors report the comoving angular distance and Hubble expansion relative to a fiducial sound horizon $r_{s,fid} = 147.78$ Mpc. In practice, our analysis uses the full covariance matrix for the BAO measurements quoted above as reported in table 8 of Alam et al. (2017). The parameter $D_V(z)$ is defined via $\equiv [D_M^2 cH^{-1}]^{1/3}$.

| Prior or Data Set | Citation |
|---|---|
| $D_V(z = 0.106)/r_s = 3.047 \pm 0.137$ | Beutler et al. (2011) |
| $D_V(z = 0.15)/r_s = 4.480 \pm 0.168$ | Ross et al. (2015) |
| $D_M(z = 0.38) r_{s,fid}/r_s = 1512 \pm 24$ Mpc | Alam et al. (2017) |
| $D_M(z = 0.51) r_{s,fid}/r_s = 1975 \pm 30$ Mpc | Alam et al. (2017) |
| $D_M(z = 0.61) r_{s,fid}/r_s = 2307 \pm 37$ Mpc | Alam et al. (2017) |
| $H(z = 0.38) r_s/r_{s,fid} = 81.2 \pm 2.4$ km/s/Mpc | Alam et al. (2017) |
| $H(z = 0.51) r_s/r_{s,fid} = 90.9 \pm 2.4$ km/s/Mpc | Alam et al. (2017) |
| $H(z = 0.61) r_s/r_{s,fid} = 99.0 \pm 2.5$ km/s/Mpc | Alam et al. (2017) |
| $100\Omega_b h^2 = 2.208 \pm 0.052$ | Cooke et al. (2016) |
| $T_{CMB} = 2.7255 \pm 0.0006$ K | Fixsen (2009) |
| redMaGiC clustering | Elvin-Poole et al. (2017) |
| redMaGiC shear profiles | Prat et al. (2017) |
| Cosmic shear | Troxel et al. (2017) |

[3]We quote the $H_0$ value obtained by the mean of the two values reported in A17. The two values in A17 differ on the $d(p,\gamma)^3$He reaction rate in the BBN calculation, and we adopted the larger of the two error bars quoted in A17.

## 3 RESULTS AND CONSISTENCY WITH EXTERNAL DATA SETS

Unless otherwise noted, we adopt a flat ΛCDM model with neutrino masses fixed at their minimal value of $\sum m_\nu = 0.06$ eV, as determined from neutrino oscillation experiments (see Lesgourgues & Pastor 2006; Olive et al. 2014, for reviews). $N_{\rm eff}$ is also held at its expected value $N_{\rm eff} = 3.046$. Holding the neutrino mass fixed is contrary to what was done in DES Collaboration (2017), where the neutrino mass was allowed to float by default. Our goal here is to measure the Hubble rate with a combined DES+BAO+BBN analysis and explore consistency in measurements of the Hubble constant within the context of this maximally restrictive cosmological model. We will, however, demonstrate that letting the neutrino mass float has a minimal impact on our measurement of the Hubble constant. In all cases, neutrino masses are modelled assuming three equally massive species.

Unless otherwise noted, consistency between two data sets is evaluated as follows. Let $p$ be the vector of model parameters shared between two experiments $A$ and $B$. We take $A$ and $B$ to be consistent with one another if the hypothesis $p_A - p_B = 0$ is acceptable. Specifically, for mutually independent experiments, we calculate

$$\chi^2 = (p_A - p_B)^{\rm T} C_{\rm tot}^{-1} (p_A - p_B) \quad (1)$$

and compute the Probability-To-Exceed (PTE) the observed value assuming the number of degrees of freedom is equal to the number of shared parameters. In the above expression, $C_{\rm tot} = C_A + C_B$ is the expected variance of the random variable $p_A - p_B$, with $C_A$ and $C_B$ being the covariance matrix of the shared cosmological parameters. Both matrices are marginalized over any additional parameters exclusive to each data set. We evaluate the PTE $P_{\chi^2}$ of the recovered $\chi^2$ value and turn it into a Gaussian-$\sigma$ using the equation

$$P_{\chi^2} = {\rm erf}\left(\frac{\text{No. of } \sigma}{\sqrt{2}}\right). \quad (2)$$

With this definition, a probability of $1 - P_{\chi^2} = 68$ per cent (95 per cent) corresponds to $1\sigma$ ($2\sigma$) difference. As a reminder, we have adopted $3\sigma$ difference ( PTE = 0.27 per cent) as our threshold for 'evidence of tension', and $5\sigma$ (PTE $= 5.96 \times 10^{-7}$) as 'definitive evidence of tension'.

Fig. 1 shows the $\Omega_{\rm m}$–$h$ degeneracy from the BAO+BBN data (blue and purple ellipses). Also shown are the corresponding constraints achieved by the DES Y1 analysis (solid curves). The two are consistent with each other at $0.6\sigma$. A joint analysis of these data sets (yellow and orange ellipses) results in

$$h = 0.674^{+0.011}_{-0.012}. \quad (3)$$

Throughout, we quote the most likely $h$ value, and the error bars are set by the 68 per cent contour of the posterior. This result is in excellent agreement with and has similar precision to that of A17 ($h = 0.674 \pm 0.013$) obtained from combining our same BAO+BBN data set with BAO measurements in the Ly $\alpha$.

We compare our posterior on $H_0$ to constraints derived from four fully independent datasets. These are as follows:

(i) *Planck* measurements of CMB anisotropies as probed by the temperature–temperature (*TT*) and low-$l$ polarization power spectra. The *Planck* TT+lowP data constrains $h$ when adopting a flat ΛCDM cosmology with minimal neutrino mass. *Planck* finds $h = 0.673 \pm 0.010$ (Planck Collaboration 2015). We note that while Planck Collaboration (2016) report updated cosmological constraints, the corresponding chains have not been released, so we have opted to restrict ourselves to the most recent public release (Planck Collaboration 2015).

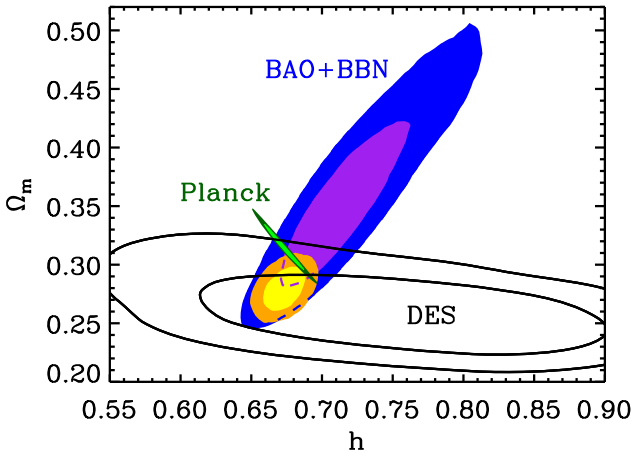


**Figure 1.** Constraints in the $\Omega_{\rm m}$–$h$ plane from the DES and BAO+BBN data as labelled. We have adopted a definition in which $\Omega_{\rm m}$ includes the contribution from massive neutrinos. All inner and outer contours enclose 68 per cent and 95 per cent of the posterior, respectively. The solid black lines show the DES $\Omega_m$–$h$ degeneracy, while the blue and purple contours show the BAO+BBN degeneracy. The DES+BAO+BBN contours are shown in yellow and orange. For reference, we have also included the corresponding contours for the *Planck* TT+lowP data set (see text).

(ii) SPTpol has measured anisotropies in the CMB via the TE and EE angular power spectra (Henning et al. 2018). In our fiducial cosmological model, they find $h = 0.712 \pm 0.021$. A similar analysis to that of Henning et al. (2018) using data from the Atacama Cosmology Telescope is presented in Louis et al. (2017). However, the corresponding uncertainties from their TE+EE data are significantly broader (see their table 4). For this analysis, we wish to restrict ourselves to data sets that constrain $H_0$ with error bars comparable to those of the SH0ES collaboration. Consequently, and in the interest of simplicity, we have focused exclusively on the (Henning et al. 2018) result. Updated analyses that combine polarization data from both SPT and ACT will be of significant interest.

(iii) The SH0ES collaboration constrains the Hubble parameter using Type Ia supernovae as standard candles. They find $h = 0.7352 \pm 0.0162$ (Riess et al. 2018). This value is an updated measurement relative to that presented in Riess et al. (2016). We note that the Riess et al. (2016) data set has been reanalysed independently in Feeney, Mortlock & Dalmasso (2018) and Follin & Knox (2018).

(iv) The H0LiCOW collaboration constrains the Hubble parameter by measuring the time delay between images of multiply imaged quasars (Bonvin et al. 2017). They find $h = 0.728 \pm 0.024$.[4]

A comparison of these various estimates of the Hubble rate and ours is shown in Fig. 2. All five measurements in Fig. 2 are effectively statistically independent and do not share observational systematics. Note in particular that the *Planck* and SPTpol data sets rely on non-overlapping $l$-ranges in the polarization spectra with

[4]Bonvin et al. (2017) report constraints both holding $\Omega_{\rm m}$ fixed and using a very wide $\Omega_{\rm m}$ prior $\Omega_{\rm m} \in [0, 1]$. We expect a reasonable prior of $\Omega_{\rm m} \in [0.2, 0.4]$ would result in a value closer to the fixed $\Omega_{\rm m}$ case and hence have chosen to use this value for our analysis, ignoring the $\Omega_{\rm m}$ dependence.

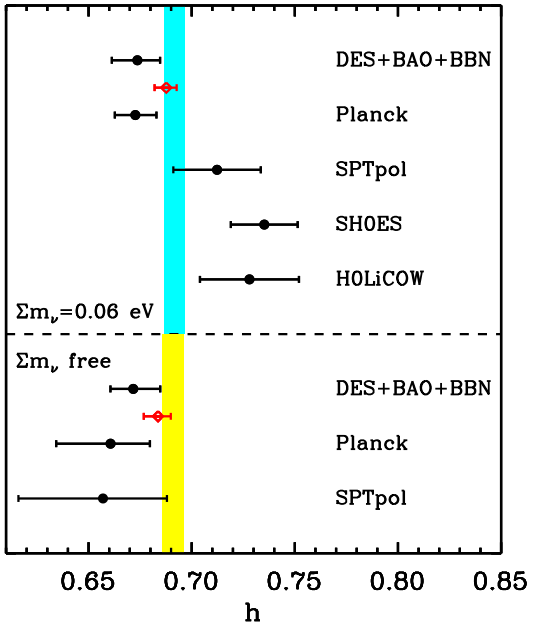


**Figure 2.** Posteriors on the Hubble parameter $h$ from five independent experiments, as labelled. Constraints above the dashed line are obtained while holding $\sum m_\nu$ fixed, while the constraints below the line allow the sum of the neutrino masses to float. In both cases, the red diamond is obtained by combining DES+BAO+BBN with *Planck*. The shift in $h$ and the greatly reduced error bars for the combined DES+BAO+BBN and *Planck* experiments reflect the degeneracy breaking illustrated in Fig. 1. The broadening and leftward shift in the $h$ posterior from CMB experiments reflects the degeneracy between $\sum m_\nu$ and $h$ in CMB observables (see text for further discussion). We emphasize that once this degeneracy is broken, all the constraints snap back into place. The cyan and yellow bands show the 68 per cent confidence region obtained when combining all five data sets for each of the two analysis (fixed and free $\sum m_\nu$). The five experiments above are statistically independent of each other and share no common observational systematics. Combining all five data sets, we arrive at $h = 0.693^{+0.004}_{-0.006}$ (fixed neutrino mass) or $h = 0.693^{+0.003}_{-0.007}$ (free neutrino mass).

minimal sky overlap (SPTpol covers only a small fraction of the *Planck* sky). While the SPTpol analysis does utilize a $\tau$ prior from *Planck*, the posterior on $h$ is insensitive to this prior: the constraint on $h$ is sensitive to the relative amplitudes and positions of the acoustic peaks, not their overall amplitude. We have explicitly verified that the SPTpol posterior on $h$ does not change when we relax the $\tau$ prior. Finally, while the *Planck* data do contain some information on local structures due to gravitational lensing, the volume overlap with the BAO and DES data sets is minimal, both because *Planck* is all-sky and because the lensing kernel for the CMB peaks at $z \approx 2$.[5]

Visually, the data points in Fig. 2 appear to be consistent with five independent realizations of a single value. We note that the two lowest $h$ values are the *Planck* and DES+BAO+BBN values. A quick look at Fig. 1 makes it obvious that when combining these two data sets, the resulting best-fitting Hubble parameter is higher than that obtained from either data set alone, improving the agreement with the remaining data sets. A combined DES+BAO+BBN+*Planck* analysis yields $h = 0.688^{+0.005}_{-0.006}$, a value higher than that of DES+BAO+BBN or *Planck* alone.[6] Consistency between DES and *Planck* was established in DES Collaboration (2017) using evidence ratios. Using the method employed in this work, we again find the two data sets to be consistent at $1.6\sigma$.

We test for the consistency of all five data sets as follows: *Planck* and SPTpol provide precise measurements of $h$, $\Omega_m$, $\Omega_b$, $\sigma_8$, and $n_s$ (10 measurements). DES+BAO+BBN measures these same parameters with the exception of $n_s$, which is not well constrained by DES. Thus, DES+BAO+BBN adds four independent measurements. Finally, SH0ES and H0LiCOW each measures $h$, for a total of 16 measurements. These are modelled using a single set of cosmological parameters (five parameters), resulting in 11 degrees of freedom. We evaluate the $\chi^2$ of the best-fitting model to the full data vector of cosmological parameter estimates, finding $\chi^2/dof = 22.6/11$. The PTE is 1.1 per cent, a $2.5\sigma$ difference. We conclude that all five data sets are consistent with each other.

We combine all five data sets to arrive at our best-fitting Hubble parameter as follows. First, we combine DES+BAO+BBN with Planck. We then evaluate the combined DES+BAO+BBN+*Planck*+SPTpol likelihood using importance sampling (see Appendix A for details). Finally, we follow a similar approach for incorporating the SH0ES and H0LiCOW constraints.[7] Combining all five data sets, we arrive at $h = 0.693^{+0.004}_{-0.006}$. This value is consistent with earlier efforts that combined CMB, SN, and BAO oscillation data and data compilations (Gaztañaga, Miquel & Sánchez 2009; Chen, Kumar & Ratra 2017).

Of the five data sets we consider, the most discrepant $H_0$ measurement is clearly that of the SH0ES collaboration. As a naive estimate of the difference between SH0ES and the remaining data sets, we combine all four non-SH0ES measurements to arrive at a best estimate of the Hubble parameter ($h = 0.688^{+0.006}_{-0.004}$). The difference between this combined value and SH0ES is $2.8\sigma$. This value fails to satisfy our criteria for evidence of tension. Moreover, because we have five different independent measurements, there is an important look-elsewhere effect. Properly estimating this effect through brute force Monte Carlo realizations of each of the five independent data sets is numerically intractable. However, we can provide a rough estimate by modelling the five measurements as independent Gaussian random draws of the same mean. For each realization, we identify the random draw that is most discrepant relative to the remaining four values. These four values are combined to form a single best estimate, and the difference between the combined result of the four most consistent draws is compared to the remaining data point using our standard test for consistency. We perform $10^5$ realizations of this numerical experiment and determine that the probability of finding a difference in excess of that observed between SH0ES and the remaining data sets is 2.4 per cent ($2.3\sigma$). If we instead combine the DES+BAO+BBN with *Planck* and SPTpol, we arrive at three independent $h$ measurements for which we can ignore the remaining cosmological parameters. The $\chi^2$ of these three independent measurements is $\chi^2/dof = 7.7/2$, corresponding to a 2.1 per cent PTE ($2.3\sigma$). In principle, this difference is also subject

[5]In principle, we could remove lensing information from *Planck* by marginalizing over the so-called $A_L$ parameter. Doing so increases the central value of the *Planck* constraint in $h$ from 0.673 to 0.689, moving *Planck* towards the combined $h$ constraint found in this work.

[6]Combining with *Planck* improves not just the constraints on $h$ but also other cosmological parameters, particularly $\sigma_8$ and $\Omega_m$. Here, we focus exclusively on $h$, as this is the key addition to the extended analysis presented in DES Collaboration (2017).

[7]Since we do not have the H0LiCOW likelihood, we have symmetrized the error bars and adopted a Gaussian likelihood. We do not expect this approximation has a large impact on the combined posterior.

to a look-elsewhere effect – we are focusing on $h$ precisely because of the *Planck* versus SH0ES comparison – so the significance of this difference should be slightly reduced.

We have also explored the impact of floating the sum of the neutrino masses in our analysis. The corresponding constraints are shown in Fig. 2, below the dashed line. Opening up neutrino masses hardly impacts the recovered Hubble constant for a DES+BAO+BBN analysis, as we would expect from the discussion in the introduction. Because CMB anisotropies are degenerate in $h$ and $\sum m_\nu$ – CMB observables are roughly constant if one increases $\sum m_\nu$ while decreasing $h$ – allowing $\sum m_\nu$ to float greatly increases the uncertainties in the recovered Hubble rate from CMB experiments. In addition, because our fiducial model corresponds to the lower limit of $\sum m_\nu$, floating $\sum m_\nu$ necessarily shifts $h$ towards lower values, as seen in Fig. 2.

The above shift is noteworthy within the broader cosmological context in that massive neutrinos have been proposed as one way to bring the clustering amplitude predicted from *Planck* in better agreement with low-redshift measurements of $S_8 = \sigma_8(\Omega_{\rm m}/0.3)^{1/2}$ (see e.g. Wyman et al. 2014). The idea is simple: Neutrinos do not cluster at small scales, so increasing the fractional contribution of neutrinos to the mass budget of the Universe decreases the predicted clustering amplitude of matter. However, such a shift must be accompanied by a lowering of the Hubble rate in order to hold CMB observables fixed. Doing so increases the difference between distance-ladder estimates of the Hubble constant and the DES+CMB constraints. That is, reducing differences in $S_8$ comes at the expense of increasing differences in $H_0$. Moreover, once we combine a CMB experiment with DES+BAO+BBN, the $\sum m_\nu$–$h$ degeneracy from CMB observables is broken, and our Hubble constant constraints snap back into place. The posterior in $h$ when combining all five data sets while letting the neutrino mass float is $h = 0.693^{+0.003}_{-0.007}$. Neutrino masses are also forced back towards their lower limit: our posterior on the neutrino mass is $\sum m_\nu < 0.18\,{\rm eV}$ (95 per cent CL).

## 4 DISCUSSION

Our combined DES+BAO+BBN analysis is similar in spirit to that of A17. In particular, whereas we break the $\Omega_{\rm m}$–$h$ degeneracy inherent to a BAO+BBN measurement using DES data, they break it using Ly $\alpha$–BAO data to find $h = 0.674 \pm 0.013$, in a perfect agreement with the earlier result by Aubourg et al. (2015).[8] We can directly incorporate Ly $\alpha$–BAO in our analysis using the Ly $\alpha \times$ Ly $\alpha$ measurements of Bautista et al. (2017) and the Ly $\alpha \times$ QSO measurements of du Mas des Bourboux et al. (2017). These results are summarized in the latter work as

$$cH^{-1}(z = 2.40)/r_{\rm s} = 8.94 \pm 0.22, \quad (4)$$

$$D_{\rm M}(z = 2.40)/r_{\rm s} = 36.6 \pm 1.2. \quad (5)$$

The difference between these values and the galaxy BAO measurements is $2.4\sigma$, increasing to $2.8\sigma$ when the DES data are added to the BAO. The addition of the Ly $\alpha$ data has a minimal impact on our constraints, resulting in a posterior $h = 0.675^{+0.011}_{-0.010}$. In principle, we could also add the recent BAO result of Ata et al. (2017), who used quasars from the eBOSS experiment to constrain the spherically averaged distance to $z = 1.52$, but the lower precision of this early eBOSS result will have no significant impact on our results.

Our DES+BAO+BBN analysis is also qualitatively similar to the inverse distance-ladder approach presented in Aubourg et al. (2015), though the underlying motivation for the analysis is rather different (an updated analysis was recently presented in Feeney et al. 2018). In Aubourg et al. (2015), the sound horizon scale $r_{\rm s}$ was calibrated using CMB data. With $r_{\rm s}$ in hand, Aubourg et al. (2015) used BAO to measure the comoving angular diameter distance to redshift $z = 0.57$, which was in turn used to calibrate the absolute magnitude of Type Ia supernova. This, in turn, allowed Aubourg et al. (2015) to use the Joint-Light curve Analysis data set of Betoule et al. (2014) to measure the local Hubble parameter directly.

Compared to our analysis, the inverse distance-ladder approach has the significant benefit of being less model dependent: The local Hubble rate is measured directly in much the same way as in the work from the SH0ES collaboration, only now the absolute magnitude calibration of the supernova is based on BAO measurements at cosmological distances.

By contrast, while our DES+BAO+BBN analysis is clearly model dependent – we have explicitly assumed a flat $\Lambda$CDM model with minimal neutrino mass – the resulting constraint on $h$ is completely independent of both CMB anisotropies and supernova data. Consequently, relative to the inverse distance ladder, we view our analysis as a cleaner test of observational systematics within the specific context of a flat $\Lambda$CDM model.

Broadly speaking, our results and conclusions mirror and update those of Bennett et al. (2014), who pursued an examination similar to this work. Like us, they find no significant evidence of tension in Hubble constant measurements, reaching a consensus value from WMAP, BAO, and SN data of $H_0 = 69.6 \pm 0.7\,{\rm km\,s^{-1}Mpc^{-1}}$. This is to be compared to our own result of $H_0 = 69.3^{+0.4}_{-0.6}\,{\rm km\,s^{-1}\,Mpc^{-1}}$. The agreement between the two values is remarkable, particularly given the various data updates, including *Planck* 2015 results for WMAP, the addition of SPTpol and DES data, and updated SN constraints.

As this paper was being completed, a similar paper appeared on the arXiv (Lin & Ishak 2017). That work compares five different estimates of $H_0$: *Planck*, SH0ES, H0LiCOW, and two more: one from BAO+BBN in conjunction with supernova, and one due to a broad variety of large-scale structure measurements, including several BAO data sets, redshift space distortion analyses, cosmic shear, and cluster abundance data. Relative to the analysis in Lin & Ishak (2017), our analysis benefits from the fact that all the probes we consider are clearly statistically independent and share no common observational systematics. While our conclusions are superficially different, we agree with their basic result: the most discrepant outlier in our collection of $H_0$ measurements is the local $H_0$ measurement from SH0ES. Our reduced estimate of the significance of this difference incorporates the look-elsewhere effects present in these type of analyses.

## 5 SUMMARY

The combination of BAO+BBN produces a tight degeneracy between $\Omega_{\rm m}$ and $h$ (Aubourg et al. 2015). Any independent probe of $\Omega_{\rm m}$ can effectively break this degeneracy, enabling a direct measurement of the Hubble parameter that is fully independent of local $H_0$ measurements and CMB anisotropies. Constraints on the matter density from lensing analyses is an especially attractive way of breaking this degeneracy: these constraints are sensitive to dark matter via its inhomogeneities, rather than through its impact on the expansion history. In that sense, they enable a holistic test of

[8] We averaged the two reported values from table 3 in A17, adding in quadrature half the difference between the two central values to the statistical error bar.

**Table 2.** Hubble parameter $h$ from the five independent data sets considered in this work, along with the best-fitting estimate coming from combining all data sets. All data sets are mutually statistically independent, and there are no shared sources of observational systematics between them. Our fiducial analysis holds $\sum m_\nu = 0.06$ eV, but we also report results obtained by marginalizing over $\sum m_\nu$.

| $h$ | Data set | Citation |
|---|---|---|
| $0.674^{+0.011}_{-0.012}$ | DES+BAO+BBN | This work |
| $0.673 \pm 0.010$ | *Planck* | Planck Collaboration (2015) |
| $0.712 \pm 0.021$ | SPTpol | Henning et al. (2018) |
| $0.7352 \pm 0.0162$ | SH0ES | Riess et al. (2018) |
| $0.728^{+0.024}_{-0.024}$ | H0LiCOW | Bonvin et al. (2017) |
| $h = 0.693^{+0.004}_{-0.006}$ | Combined | This work |
| $h = 0.672^{+0.013}_{-0.011}$ | DES+BAO+BBN ($\sum m_\nu$ free) | This work |
| $h = 0.693^{+0.003}_{-0.007}$ | Combined ($\sum m_\nu$ free) | This work |

the Big Bang theory that probes not just the expanding Universe framework, but also our understanding of density perturbations in the Universe.

We have used the recent DES Y1 data set to place a precise measurement of the Hubble constant by combining it with BAO and BBN data (Drlica-Wagner et al. 2017; Zuntz et al. 2017). We find $H_0 = 67.4^{+1.1}_{-1.2}$ km s$^{-1}$ Mpc$^{-1}$.Our result is in 2.8$\sigma$ difference with Ly $\alpha$–BAO measurements, though the combined galaxy and Ly $\alpha$–BAO measurements are in good agreement with DES. Adding Ly $\alpha$–BAO data to our DES+BAO+BBN measurement has minimal impact on our results. While our fiducial analysis holds the sum of neutrino masses fixed, marginalizing over neutrino mass does not significantly relax our constraint on the Hubble constant.

We have compared our measurement of $H_0$ to four additional experimental values of comparable precision (see Table 2): *Planck* TT+lowP measurements of $H_0$ assuming a flat $\Lambda$CDM model of minimal neutrino mass; SPTpol measurements of $H_0$ in the same cosmological model; the local supernovae-based distance ladder measurement of $H_0$ from the SH0ES collaboration (Riess et al. 2018); and the H0LiCOW measurement using multiply imaged quasars from Bonvin et al. (2017). All five measurements are mutually statistically independent of each other, and there are no shared observational systematics between them. Amongst these five, the most discrepant data set is that of the SH0ES collaboration, which is in 2.8$\sigma$ difference with the remaining four experiments. We estimate the probability of finding a fluctuation this large or larger in a set of five independent measurements to be 2.4 per cent, a 2.3$\sigma$ fluctuation. Viewed in this broader context, the $H_0$ value from the SH0ES collaboration is less problematic.

Importantly, all $H_0$ measurements used in this work are expected to improve in precision in the coming years. Future CMB experiments such as Advanced ACTPol (De Bernardis et al. 2016), SPT-3G (Benson et al. 2014), and CMB-S4 (Abitbol et al. 2017) will survey an order of magnitude more sky area with factors of several lower noise than SPTpol. By resolving the acoustic oscillations in the damping tail in the polarization power spectra of the CMB, these experiments will eventually surpass Planck in terms of their ability to constrain cosmological parameters, including $h$ (Galli et al. 2014). Likewise, the DES survey area will more than triple, while doubling the integrated exposure per galaxy. Future surveys such as the LSST (LSST Science Collaboration. 2009) will further improve upon the DES five year constraints. BAO constraints from eBOSS (Dawson et al. 2016) will increase the galaxy BAO measurements to redshifts $z\sim 1$, only to be surpassed by new spectroscopic surveys such as DESI (DESI Collaboration 2016a,b) and the Taipan Galaxy Survey (da Cunha et al. 2017) shortly, thereafter. Local $H_0$ measurements will improve with improved distance calibration from Gaia (Gaia Collaboration 2016), and innovative techniques such as using the tip of the red giant branch to build the distance ladder (Freedman 2017). Finally, continued monitoring and improved lens modelling techniques will further reduce the uncertainty of strong-lens estimates of $H_0$. Together, these improvements along with new measurements from gravitational wave events (Abbott et al. 2017) will lead to ever more stringent tests of the Big Bang model and the currently standard flat $\Lambda$CDM model across its full 13.8 billion yr history.

## ACKNOWLEDGEMENTS

This paper has gone through internal review by the DES collaboration. ER is supported by DOE grant DE-SC0015975 and by the Sloan Foundation, grant FG-2016-6443. YP is supported by DOE grant DE-SC0015975. Funding for the DES Projects has been provided by the U.S. Department of Energy, the U.S. National Science Foundation, the Ministry of Science and Education of Spain, the Science and Technology Facilities Council of the United Kingdom, the Higher Education Funding Council for England, the National Center for Supercomputing Applications at the University of Illinois at Urbana-Champaign, the Kavli Institute of Cosmological Physics at the University of Chicago, the Center for Cosmology an d Astro-Particle Physics at the Ohio State University, the Mitchell Institute for Fundamental Physics and Astronomy at Texas A&M University,Financiadora de Estudos e Projetos, Fundação Carlos Chagas Filho de Amparo à Pesquisa do Estado do Rio de Janeiro, Conselho Nacional de Desenvolvimento Científico e Tecnológico and the Ministério da Ciência, Tecnologia e Inovação, the Deutsche Forschungsgemeinschaft, and the Collaborating Institutions in the DES.

The Collaborating Institutions are Argonne National Laboratory, the University of California at Santa Cruz, the University of Cambridge, Centro de Investigaciones Energéticas, Medioambientales y Tecnológicas-Madrid, the University of Chicago, University College London, the DES-Brazil Consortium, the University of Edinburgh, the Eidgenössische Technische Hochschule (ETH) Zürich, Fermi National Accelerator Laboratory, the University of Illinois at Urbana-Champaign, the Institut de Ciències de l'Espai (IEEC/CSIC), the Institut de Física d'Altes Energies, Lawrence Berkeley National Laboratory, the Ludwig-Maximilians Universität München and the associated Excellence Cluster Universe, the University of Michigan, the National Optical Astronomy Observatory, the University of Nottingham, The Ohio State University, the University of Pennsylvania, the University of Portsmouth, SLAC National Accelerator Laboratory, Stanford University, the University of Sussex, Texas A&M University, and the OzDES Membership Consortium.

Based in part on observations at Cerro Tololo Inter-American Observatory, National Optical Astronomy Observatory, which is operated by the Association of Universities for Research in Astronomy (AURA) under a cooperative agreement with the National Science Foundation.

The DES data management system is supported by the National Science Foundation under Grant Numbers AST-1138766 and AST-1536171. The DES participants from Spanish institutions

are partially supported by MINECO under grants AYA2015-71825, ESP2015-66861, FPA2015-68048, SEV-2016-0588, SEV-2016-0597, and MDM-2015-0509, some of which include ERDF funds from the European Union. IFAE is partially funded by the CERCA program of the Generalitat de Catalunya. Research leading to these results has received funding from the European Research Council under the European Union's Seventh Framework Program (FP7/2007-2013) including ERC grant agreements 240672, 291329, and 306478. We acknowledge support from the Australian Research Council Centre of Excellence for All-sky Astrophysics (CAASTRO), through project number CE110001020.

The South Pole Telescope program is supported by the National Science Foundation through grant PLR-1248097. Partial support is also provided by the NSF Physics Frontier Center grant PHY-0114422 to the Kavli Institute of Cosmological Physics at the University of Chicago, the Kavli Foundation, and the Gordon and Betty Moore Foundation through Grant GBMF#947 to the University of Chicago.

This manuscript has been authored by Fermi Research Alliance, LLC under Contract No. DE-AC02-07CH11359 with the U.S. Department of Energy, Office of Science, Office of High Energy Physics. The United States Government retains and the publisher, by accepting the article for publication, acknowledges that the United States Government retains a non-exclusive, paid-up, irrevocable, world-wide license to publish or reproduce the published form of this manuscript, or allow others to do so, for United States Government purposes.

## REFERENCES

Abbott B. P. et al., 2017, Nature, 551, 85
Abitbol M. H. et al., 2017, preprint (arXiv:1706.02464)
Addison G. E., Hinshaw G., Halpern M., 2013, MNRAS, 436, 1674
Addison G. E., Watts D. J., Bennett C. L., Halpern M., Hinshaw G., Weiland J. L., 2017, ApJ, 853, 119
Alam S. et al., 2017, MNRAS, 470, 2617
Alsing J., Heavens A., Jaffe A. H., 2017, MNRAS, 466, 3272
Ata M. et al., 2017, MNRAS, 473, 4773
Aubourg É. et al., 2015, Phys. Rev. D, 92, 123516
Bautista J. E. et al., 2017, A&A, 603, A12
Bennett C. L., Larson D., Weiland J. L., Hinshaw G., 2014, ApJ, 794, 135
Benson B. A. et al., 2014, in Proc. SPIE Conf. Ser. Vol. 9153, Millimeter, Submillimeter, and Far-Infrared Detectors and Instrumentation for Astronomy VII. SPT-3G: a next-generation cosmic microwave background polarization experiment on the South Pole telescope. SPIE, Bellingham, p. 91531P
Betoule M. et al., 2014, A&A, 568, A22
Beutler F. et al., 2011, MNRAS, 416, 3017
Bonvin V. et al., 2017, MNRAS, 465, 4914
Cawthon R. et al., 2017, preprint (arXiv:1712.07298)
Chen Y., Kumar S., Ratra B., 2017, ApJ, 835, 86
Cooke R. J., Pettini M., Nollett K. M., Jorgenson R., 2016, ApJ, 830, 148 (C16)
da Cunha E. et al., 2017, Publ. Astron. Soc. Aust., 34, e047
Davis C. et al., 2017, preprint (arXiv:1710.02517)
Dawson K. S. et al., 2016, AJ, 151, 44
De Bernardis F. et al., 2016, in Proc. SPIE Conf. Ser. Vol. 9910, Observatory Operations: Strategies, Processes, and Systems VI. SPIE, Bellingham. p. 991014
DES Collaboration, 2017, preprint (arXiv:1708.01530)
DESI Collaboration, 2016a, preprint (arXiv:1611.00036)
DESI Collaboration, 2016b, preprint (arXiv:1611.00037)
Drlica-Wagner A. et al., 2017, ApJS, 235, 33
du Mas des Bourboux H. et al., 2017, A&A, 608, A130
Elvin-Poole J. et al., 2017, preprint (arXiv:1708.01536)
Feeney S. M., Mortlock D. J., Dalmasso N., 2018, MNRAS, 476, 3861
Feeney S. M., Peiris H. V., Williamson A. R., Nissanke S. M., Mortlock D. J., Alsing J., Scolnic D., 2018, preprint (arXiv:e-prints)
Fields B. D., Molaro P., Sarkar S., 2014, preprint (arXiv:1412.1408)
Fixsen D. J., 2009, ApJ, 707, 916
Follin B., Knox L., 2018, MNRAS, 477, 4534
Freedman W. L., 2017, Nature Astron., 1, 0121
Freedman W. L. et al., 2012, ApJ, 758, 24
Gaia Collaboration, 2016, A&A, 595, A1
Galli S. et al., 2014, Phys. Rev. D, 90, 063504
Gatti M. et al., 2017, MNRAS, 477, 1664
Gaztañaga E., Cabré A., Hui L., 2009, MNRAS, 399, 1663
Gaztañaga E., Miquel R., Sánchez E., 2009, Phys. Rev. Lett., 103, 091302
Henning J. W. et al., 2018, ApJ, 852, 97
Hildebrandt H. et al., 2017, MNRAS, 465, 1454
Hoyle B. et al., 2017, MNRAS, 478, 592
Krause E. et al., 2017, preprint (arXiv:1706.09359)
Lesgourgues J., Pastor S., 2006, Phys. Rep., 429, 307
Lewis A., Bridle S., 2002, Phys. Rev. D, 66, 103511
Lin W., Ishak M., 2017, Phys. Rev. D, 96, 083532
Louis T. et al., 2017, JCAP, 6, 031
LSST Science Collaboration, 2009, preprint (arXiv:0912.0201)
MacCrann N. et al., 2018, preprint (arXiv:1803.09795)
Mandelbaum R. et al., 2013, MNRAS, 432, 1544
Olive K. A. et al., 2014, Chin. Phys., 38, 090001
Planck Collaboration, 2015, A&A, 594, A14
Planck Collaboration, 2016, A&A, 596, A107
Prat J. et al., 2017, preprint (arXiv:1708.01537)
Riess A. G. et al., 2016, ApJ, 826, 56
Riess A. G. et al., 2018, ApJ, 861, 126
Ross A. J., Samushia L., Howlett C., Percival W. J., Burden A., Manera M., 2015, MNRAS, 449, 835
Rozo E. et al., 2016, MNRAS, 461, 1431
Troxel M. A. et al., 2017, preprint (arXiv:1708.01538)
Troxel M. A. et al., 2018, MNRAS, 479, 4998
van Uitert E. et al., 2017, MNRAS, 476, 4662
Weinberg S., 1989, Rev. Mod. Phys., 61, 1
Wyman M., Rudd D. H., Vanderveld R. A., Hu W., 2014, Phys. Rev. Lett., 112, 051302
Zuntz J. et al., 2015, Astron. Comput., 12, 45
Zuntz J. et al., 2017, preprint (arXiv:1708.01533)

## APPENDIX A: IMPORTANCE SAMPLING WITH NUISANCE PARAMETERS

The SPTpol likelihood was written as a `CosmoMC` (Lewis & Bridle 2002) module, whereas the DES likelihood was written as a `CosmoSIS` (Zuntz et al. 2015) module. This difference makes it difficult to run a combined chain. Consequently, we rely on importance sampling, evaluating the SPTpol likelihood at each of the links of the DES+BAO+BBN+*Planck* chains. However, the SPTpol likelihood includes several nuisance parameters, including the two which are not prior dominated: $A_{80}^{\rm EE}$, the EE dust amplitude; and $D_{3000}^{\rm PS_{EE}}$, the EE Poisson foreground amplitude. One must correctly account for these nuisance parameters in the calculation. We describe how we do so here.

Consider two experiments $A$ and $B$. The two experiments share a set of parameters $p$, but each experiment additionally contains a set of nuisance parameters exclusive to itself, namely $q_A$ and $q_B$. Given an arbitrary function $f(p, q_A, q_B)$, we wish to be able to evaluate

$$\langle f \rangle = \int {\rm d}p{\rm d}q_A{\rm d}q_B \; L_A(p, q_A) L_B(p, q_B) \times P_0(p) P_0(q_A) P_0(q_B) f(p, q_A, q_B), \quad \text{(A1)}$$

Where $L_X$ is the likelihood for experiment $X$ and $P_0$ represents the priors for different parameter sets. We assume here that the experiments are independent of each other, and that the priors on $p$, $q_A$, and $q_B$ are separable.

We wish to importance sample MCMC results from experiment A using the likelihood from experiment B. In order to efficiently sample the parameter space spanned by $q_B$, we multiply and divide the integrand by $G(q_B)$, where $G$ is a probability distribution chosen to be wider than the posterior of $q_B$ (as estimated from the chains of experiment $B$ alone). We can rewrite the above expression as

$$\langle f \rangle = \int \mathrm{d}p\mathrm{d}q_A\mathrm{d}q_B \; [L_A(p, q_A)P_0(p)P_0(q_A)P_0(q_B)G(q_B)] \times \left[\frac{L_B(p, q_B)}{G(q_B)} f(p, q_A, q_B)\right] = \left\langle \frac{L_B}{G} f \right\rangle_A , \quad \text{(A2)}$$

where the last expectation value refers to evaluating the expectation value of the function $fL_B/G$ over the distribution $L_A(p, q_A)P_0(p)P_0(q_A)P_0(q_B)G(q_B)$. Note this distribution is separable in ($p$,$q_A$), and $q_B$. Random draws from $L_A(p, q_A)P_0(p)P_0(q_A)$ are given by the chain from experiment $A$, while we can readily sample from the distribution $P_0(q_B)G(q_B)$. To decrease the numerical noise of the integration over the nuisance parameters, we sample 20 different sets of $q_B$ values for each link in $p$. We found this was sufficient to achieve good convergence and explicitly tested using chains with both half as many points and twice as many points.

In short, to importance sample the SPTpol likelihood, we first oversample the DES chain according to the weights. For each link, we assign nuisance parameters for SPTpol by randomly drawing from the distribution $P_0(q_B)G(q_B)$. Each link is then assigned a weight of $L_B/G$.

Finally, to achieve more efficient sampling of the posterior of the combined DES+BAO+BBN+*Planck*+SPTpol chain, we further modified our method as follows. First, we used the SPTpol chain to compute the parameter covariance matrix. We use this to define a Gaussian approximation $G_{\rm SPT}$ to the SPT likelihood. This Gaussian approximation is then included in the DES+BAO+BBN+*Planck* chain, and the assigned weight to each link becomes $L_{\rm SPT}/(G \times G_{\rm SPT})$.

[1]*Cerro Tololo Inter-American Observatory, National Optical Astronomy Observatory, Casilla 603, La Serena, Chile*
[2]*Department of Physics and Electronics, Rhodes University, PO Box 94, Grahamstown 6140, South Africa*
[3]*Department of Physics & Astronomy, University College London, Gower Street, London WC1E 6BT, UK*
[4]*Fermi National Accelerator Laboratory, P. O. Box 500, Batavia, IL 60510, USA*
[5]*LSST, 933 North Cherry Avenue, Tucson, AZ 85721, USA*
[6]*Department of Astronomy and Astrophysics, University of Chicago, Chicago, IL 60637, USA*
[7]*Kavli Institute for Cosmological Physics, University of Chicago, Chicago, IL 60637, USA*
[8]*Observatories of the Carnegie Institution of Washington, 813 Santa Barbara St, Pasadena, CA 91101, USA*
[9]*Department of Physics and Astronomy, University of Pennsylvania, Philadelphia, PA 19104, USA*
[10]*CNRS, UMR 7095, Institut d'Astrophysique de Paris, F-75014 Paris, France*
[11]*Sorbonne Universités, UPMC Univ Paris 06, UMR 7095, Institut d'Astrophysique de Paris, F-75014 Paris, France*
[12]*Kavli Institute for Particle Astrophysics & Cosmology, P. O. Box 2450, Stanford University, Stanford, CA 94305, USA*
[13]*SLAC National Accelerator Laboratory, Menlo Park, CA 94025, USA*
[14]*Observatório Nacional, Rua Gal. José Cristino 77, Rio de Janeiro RJ - 20921-400, Brazil*
[15]*Laboratório Interinstitucional de e-Astronomia - LIneA, Rua Gal. José Cristino 77, Rio de Janeiro RJ - 20921-400, Brazil*
[16]*Department of Astronomy, University of Illinois, 1002 W. Green Street, Urbana, IL 61801, USA*
[17]*National Center for Supercomputing Applications, 1205 West Clark St., Urbana, IL 61801, USA*
[18]*Institut de Física d'Altes Energies (IFAE), The Barcelona Institute of Science and Technology, Campus UAB, E-08193 Bellaterra (Barcelona), Spain*
[19]*Institute of Space Sciences, IEEC-CSIC, Campus UAB, Carrer de Can Magrans, s/n, E-08193 Barcelona, Spain*
[20]*High Energy Physics Division, Argonne National Laboratory, 9700 S. Cass Avenue, Argonne, IL 60439, USA*
[21]*Department of Physics, IIT Hyderabad, Kandi, Telangana 502285, India*
[22]*Faculty of Physics, Ludwig-Maximilians-Universität, Scheiner str 1, D-81679 Munich, Germany*
[23]*Excellence Cluster Universe, Boltzmannstr. 2, D-85748 Garching, Germany*
[24]*Department of Astronomy, University of Michigan, Ann Arbor, MI 48109, USA*
[25]*Department of Physics, University of Michigan, Ann Arbor, MI 48109, USA*
[26]*Instituto de Fisica Teorica UAM/CSIC, Universidad Autonoma de Madrid, E-28049 Madrid, Spain*
[27]*Universitäts-Sternwarte, Fakultät für Physik, Ludwig-Maximilians Universität München, Scheiner str 1, D-81679München, Germany*
[28]*Institute of Astronomy, University of Cambridge, Madingley Road, Cambridge CB3 0HA, UK*
[29]*Kavli Institute for Cosmology, University of Cambridge, Madingley Road, Cambridge CB3 0HA, UK*
[30]*Department of Physics, ETH Zurich, Wolfgang-Pauli-Strasse 16, CH-8093 Zurich, Switzerland*
[31]*Department of Physics, The Ohio State University, Columbus, OH 43210, USA*
[32]*Center for Cosmology and Astro-Particle Physics, The Ohio State University, Columbus, OH 43210, USA*
[33]*Max Planck Institute for Extraterrestrial Physics, Giessenbachstrasse, D-85748 Garching, Germany*
[34]*Astronomy Department, University of Washington, Box 351580, Seattle, WA 98195, USA*
[35]*Santa Cruz Institute for Particle Physics, Santa Cruz, CA 95064, USA*
[36]*Jet Propulsion Laboratory, California Institute of Technology, 4800 Oak Grove Dr., Pasadena, CA 91109, USA*
[37]*Australian Astronomical Observatory, North Ryde NSW 2113, Australia*
[38]*Argonne National Laboratory, 9700 South Cass Avenue, Lemont, IL 60439, USA*
[39]*Institute for Astronomy, University of Edinburgh, Edinburgh EH9 3HJ, UK*
[40]*Departamento de Física Matemática, Instituto de Física, Universidade de São Paulo, CP 66318, São Paulo SP 05314-970, Brazil*
[41]*Institut d'Astrophysique de Paris, F-75014 Paris, France*
[42]*Department of Physics and Astronomy, George P. and Cynthia Woods Mitchell Institute for Fundamental Physics and Astronomy, Texas A&M University, College Station, TX 77843, USA*
[43]*Institució Catalana de Recerca i Estudis Avançats, E-08010 Barcelona, Spain*
[44]*Dunlap Institute for Astronomy and Astrophysics, University of Toronto, 50 St George St, Toronto ON M5S 3H4, Canada*
[45]*Lawrence Berkeley National Laboratory, 1 Cyclotron Road, Berkeley, CA 94720, USA*
[46]*Department of Physics, University of Arizona, Tucson, AZ 85721, USA*
[47]*School of Physics, University of Melbourne, Parkville VIC 3010, Australia*
[48]*Centro de Investigaciones Energéticas, Medioambientales y Tecnológicas (CIEMAT), Madrid, Spain*

[49] *School of Physics and Astronomy, University of Southampton, Southampton SO17 1BJ, UK*
[50] *Instituto de Física Gleb Wataghin, Universidade Estadual de Campinas, 13083-859, SP, Campinas, Brazil*
[51] *Computer Science and Mathematics Division, Oak Ridge National Laboratory, Oak Ridge, TN 37831, USA*
[52] *Institute of Cosmology & Gravitation, University of Portsmouth, Portsmouth PO1 3FX, UK*
[53] *Department of Physics, Stanford University, 382 Via Pueblo Mall, Stanford, CA 94305, USA*
[54] *Brookhaven National Laboratory, Bldg 510, Upton, NY 11973, USA*
[55] *Institute of Physics, Laboratory of Astrophysics, École Polytechnique Fédérale 55 de Lausanne (EPFL), Observatoire de Sauverny, 1290 Versoix, Switzerland*

This paper has been typeset from a TEX/LATEX file prepared by the author.